

## Effects of long-range and short-range order on the electronic structure of CsCl-type model alloys

Masao Nakao and Masao Doyama

*Department of Metallurgy and Materials Science, Faculty of Engineering,  
The University of Tokyo, Bunkyo-ku, Tokyo 113, Japan*

(Received 8 March 1979)

A new self-consistent scheme including long-range and short-range order parameters is derived from extending the idea of the single-site coherent-potential approximation in order to investigate the electronic structure of CsCl-type order-disorder alloys. The theory is based on two models; one is a usual tight-binding model with only the first-nearest-neighbor hopping integral (model I), and the other is the one in which the hopping integrals between the second and higher neighbors are approximately taken into account (model II). Numerical results are obtained with the help of a continued-fraction technique. To demonstrate the feasibility of the present method, the change in the density-of-states (DOS) curves as a function of the degree of order is shown and discussed. It is interesting to note that their general shapes for both models are quite different, i.e., model I gives a symmetric DOS curves, while model II gives an asymmetric one. We conclude that the inclusion of the second-neighbor hopping integral is especially important in CsCl-type alloys.

### I. INTRODUCTION

A large number of extensions and applications have been made on the coherent-potential approximation (CPA)<sup>1</sup> in the last decade. Some of them were concerned with what we call cluster effects. The original CPA was constructed for completely disordered systems within the framework of the single-site approximation. Therefore, it cannot take into account the fluctuations in the atomic distribution, nor investigate the effects in the presence of atomic correlation or partial order of configurations. In one-dimensional systems, Tsukada<sup>2</sup> proposed the cellular CPA which applied the CPA formalism not to a single site but to a cluster, or a cell of sites. The numerical results were found to agree with the computer simulations by Dean<sup>3</sup> for all concentrations. However, its extension to three-dimensional systems is not straightforward because of the difficulty of calculation and besides the lack of a general prescription to divide the whole system into repeating equivalent cells which should have the full symmetry required by the lattice structure. Brouers *et al.*<sup>4</sup> considered a compact cluster formed by a central atom surrounded by its  $Z$  nearest neighbors embedded in an effective medium and derived an approximate self-consistent scheme (referred to as cluster CPA hereafter). In this method, the effective medium is so determined that the scattering from the cluster is zero on the assumption that the effects of local environment depend only on the number of each type of nearest-neighbor atoms and not on their configuration. The validity of this assumption was investigated in the

simple cubic (sc) lattice by Miwa.<sup>5</sup> It should be noted that this scheme is not the same as the cellular CPA, because it does not depend on whether the system can be divided into these clusters or not. This fact makes it difficult to estimate the validity of the approximation, but enables us to apply the cluster CPA to a variety of systems. Especially, it has been applied successfully to the investigation of the effects of local environment on the magnetic and electronic properties of alloys.<sup>6</sup>

The self-consistent condition proposed by Brouers *et al.* could be regarded as the extension of the central-site approximation of Butler's paper<sup>7</sup> to three-dimensional systems. Nickel and Butler pointed out that the Green's function in the central-site approximation was not an analytic function of the energy parameter  $z$  in a strong-scattering regime.<sup>8</sup> In addition, a recent paper has reported that the boundary-site approximation, which is identical to the cellular CPA in one dimension, also fails to give analytic results for three-dimensional systems in the strong-scattering regime.<sup>9</sup> These difficulties tend to appear generally when the cluster effects are eminent. However, it is known that, in 50-50% binary alloys, the cluster effects are small and even the single-site CPA accounts quite well for the overall band shape.<sup>10,11</sup> As we are to deal with such systems, this nonanalyticity problem is not so serious.

Another category of the extension related to the cluster effects is to incorporate the atomic correlation into the theory. This extension is required from two points of view. First, real alloys would always have, more or less, some sort of local order, i.e., a tenden-

cy to segregate or to make a compound. Thus, we have to investigate the effects of local order on physical quantities when we try to make an explicit comparison with experiments. Second, in order to construct a band theory for order-disorder phase transformations, it is the first step to make a band model available for every degree of order. Theoretical progress in this direction can be summarized as follows: We define certain parameters  $\{\alpha_i\}$  ( $i = 1, 2, \dots, n$ ) which measure multisite correlations, e.g., long-range order (LRO), short-range order (SRO), three-body correlations, etc. These parameters  $\{\alpha_i\}$ , called order parameters, specify the atomic configurations to choose as a member of ensemble when we carry out the configurational ensemble average. For example, in a finite system consisting of  $N_A A$  and  $N_B B$  atoms, there are  $(N_A + N_B)! / (N_A! N_B!)$  possible configurations and in the case of perfect disorder, we must regard all of them as members of the ensemble. Each of these possible configurations has some value for the set of parameters  $\{\alpha_i\}$  and they can be classified according to their values of  $\{\alpha_i\}$ . Provided that the parameters are properly chosen, the systems with the same value of  $\{\alpha_i\}$  should give the same electronic contribution to the free energy of the electronic-ion system. In other words, the probability of every configuration classified into the same class should be equal. This condition enables us to carry out the configurational and the thermodynamical averages independently. Then, our problem can be separated into two parts; (i) we investigate the averaged electronic properties such as the total energy in the class of configurations labeled by  $\{\alpha_i\}$  and (ii) the equilibrium value of  $\{\alpha_i\}$  is determined as a function of temperature by minimizing the free energy which contains the configurational entropy associated with the class.

Thus far, the improvements along this line have always been concerned with either LRO or SRO. Foo and Amar<sup>12</sup> employed a modification of the single-site CPA and calculated the electronic DOS in one-dimensional systems with LRO [referred to as CPA( $\eta$ ) hereafter;  $\eta$  is the LRO parameter defined later]. Plischke and Mattis<sup>13</sup> compared the moments of this CPA( $\eta$ ) DOS with the exact ones found that for any value of the potential and  $\eta$ , CPA( $\eta$ ) reproduced at least the first eight moments correctly. On the other hand, for SRO, it is necessary to make use of the cluster theories because of its pair-site nature. There have been a number of SRO theories,<sup>14-18</sup> one of which is the modification of the cluster CPA<sup>19</sup> referred to as CCPA( $\sigma$ ) ( $\sigma$  is the SRO parameter defined later). However, it has been pointed out that convergence difficulties occur for large absolute values of the SRO parameter because the description of partially ordered states by a unique effective medium is less justified when the degree of order increases. Therefore, we cannot use the CCPA( $\sigma$ ) for

a band theory of order-disorder transformations. For a better description of partially ordered states, we would need to incorporate both LRO and SRO together and moreover other multisite correlations, if possible.

Now, the foregoing remarks lead us to an idea of combining the CCPA( $\sigma$ ) with the CPA( $\eta$ ) to obtain an approximate self-consistent scheme which includes both  $\sigma$  and  $\eta$  as given parameters. [We call this CCPA( $\eta, \sigma$ ).] Our method can be applied to every type of order-disorder alloy at least in principle, but, in this paper, we shall confine ourselves to CsCl-type order-disorder alloys for simplicity. The explicit form of our self-consistent scheme is derived in Sec. II. Using this method, we are able to investigate, for example, the effects of local environment on the electronic structure of alloys exhibiting both LRO and SRO. Some illustrative examples of numerical results are shown and discussed in Sec. III. Section IV contains concluding remarks.

## II. THEORY

We consider a transition-metal alloy  $A_{0.5}B_{0.5}$  whose crystalline structure is bcc in the disordered state and CsCl-type in the ordered state. As a simple model for  $d$  bands of this alloy, the usual tight-binding Hamiltonian is used. This model has essential features required for a self-consistent treatment of charge transfers and intersite and intrasite electron-electron Coulomb interactions which are believed to be important factors for order-disorder phase transformations. The one-electron Hamiltonian is then given by

$$\hat{H} = \sum_i |i\rangle \epsilon_i \langle i| + \sum_{i \neq j} |i\rangle h_{ij} \langle j|, \quad (1)$$

where the state  $|i\rangle$  is the Wannier state centered at the site  $i$  and  $\epsilon_i$  is a random-site energy which can take two values,  $\epsilon_A$  and  $\epsilon_B$ , depending on whether the site  $i$  is occupied by an  $A$  or a  $B$  atom, respectively. The site energy  $\epsilon_i$  would be generally dependent on the local environment around the site  $i$  and, moreover, would vary with ordering.<sup>20</sup> In this paper, however, these corrections are ignored.  $h_{ij}$  is a hopping integral between the site  $i$  and the site  $j$  assumed to be independent of the chemical nature of atoms. The effect of random  $h_{ij}$  called off-diagonal randomness can be easily handled under Shiba's condition<sup>21-23</sup> although it is a quite arbitrary and restrictive condition. For simplicity, we neglect the degeneracy of the  $d$  states, which is not essential for our present purpose.

To incorporate the LRO correlation, the bcc lattice is divided into two equivalent sc sublattices labeled by  $\alpha$  and  $\beta$  according to the definition of LRO. In general, LRO parameter  $\eta$  is defined (also for non-

stoichiometric compounds) by

$$\eta = \frac{N_A^\alpha + N_B^\beta - N_A^\beta - N_B^\alpha}{N_0} \quad (2)$$

where  $N_A^\alpha$ , for example, represents the number of  $A$  atoms within the  $\alpha$  sublattice and  $N_0$  is the total number of atoms. We regard the bcc lattice as the sc lattice with two atoms in a unit cell, so that the Wannier states can be rewritten as  $|n\alpha\rangle$  and  $|n\beta\rangle$ , using the cell index  $n$  which runs over the sc lattice points instead of the site index  $i$ . Then, the Hamiltonian (1) becomes

$$\begin{aligned} \hat{H} = & \sum_n |n\alpha\rangle \epsilon_{n\alpha} \langle n\alpha| + \sum_{n \neq m} |n\alpha\rangle h_{n\alpha, m\alpha} \langle m\alpha| \\ & + \sum_n |n\beta\rangle \epsilon_{n\beta} \langle n\beta| + \sum_{n \neq m} |n\beta\rangle h_{n\beta, m\beta} \langle m\beta| \\ & + \sum_{n, m} (|n\alpha\rangle h_{n\alpha, n\beta} \langle m\beta| + |n\beta\rangle h_{n\beta, m\alpha} \langle m\alpha|) \quad (3) \end{aligned}$$

In the framework of the CPA ( $\eta$ ), averaged properties of this alloy are described by an effective Hamiltonian  $\hat{H}_{\text{eff}}$  with uniform, energy-dependent and complex site energies,  $\Sigma_\alpha(z)$  and  $\Sigma_\beta(z)$ , which have to be determined self-consistently. As we are concerned with one-particle properties, it is necessary to calculate the configurational average of the Green's function, which is written

$$\hat{G} = \langle (z - \hat{H})^{-1} \rangle_c = (z - \hat{H}_{\text{eff}})^{-1} \quad (4)$$

It is convenient to perform the calculation in the Bloch representation, using a basis  $|\bar{k}\rangle = (|\bar{k}\alpha\rangle, |\bar{k}\beta\rangle)$ ;

$$|\bar{k}\alpha\rangle = \left( \frac{1}{N} \right)^{1/2} \sum_n \exp(i\bar{k} \cdot \bar{r}_n) |n\alpha\rangle \quad (5a)$$

$$|\bar{k}\beta\rangle = \left( \frac{1}{N} \right)^{1/2} \sum_n \exp(i\bar{k} \cdot \bar{r}_n) |n\beta\rangle \quad (5b)$$

where  $N$  denotes the number of unit cells or the number of sites within each sublattice here and  $\bar{r}_n$  is a sc lattice vector corresponding to the cell  $n$ . Due to our regarding the bcc lattice as the sc lattice with two atoms in a unit cell,  $\bar{k}$  is a wave vector inside the first Brillouin zone not of the bcc but of the sc lattice structure. Then, the averaged Green's function, is a  $2 \times 2$  matrix quantity in the  $\bar{k}$  representation, can be written in the form

$$\begin{aligned} G(\bar{k}, z) = & \langle \bar{k} | \hat{G}(z) | \bar{k} \rangle \\ = & \begin{pmatrix} z - \Sigma_\alpha - S(\bar{k}) & -\exp(i\bar{k} \cdot \bar{a}) \cdot \Gamma(\bar{k}) \\ -\exp(-i\bar{k} \cdot \bar{a}) \cdot \Gamma(\bar{k}) & z - \Sigma_\beta - S(\bar{k}) \end{pmatrix}^{-1} \\ \equiv & G[S(\bar{k}), \Gamma(\bar{k}), z] \quad (6) \end{aligned}$$

where  $\bar{a}$  is an arbitrary lattice vector between the first

nearest neighbors, i.e.,  $\alpha$  and  $\beta$  sites in a unit cell.  $S(\bar{k})$  and  $\Gamma(\bar{k})$  are given by

$$S(\bar{k}) = \sum_{n(\neq 0)} h_{n\alpha, 0\alpha} \exp[i\bar{k} \cdot (\bar{r}_{n\alpha} - \bar{r}_{0\alpha})] \quad (7a)$$

$$\Gamma(\bar{k}) = \sum_n h_{n\alpha, 0\beta} \exp[i\bar{k} \cdot (\bar{r}_{n\alpha} - \bar{r}_{0\beta})] \quad (7b)$$

It is worthwhile noting that when the summation is taken only over the nearest neighbors,  $S(\bar{k})$  and  $\Gamma(\bar{k})$  have the same form as the sc and the bcc dispersion relations of nearest-neighbor tight-binding metals, respectively.

To simplify the numerical computation,  $S(\bar{k})$  will be assumed to be the following forms: (model I)

$$S(\bar{k}) \approx 0 \quad (8a)$$

(model II)

$$S(\bar{k}) \approx \frac{1}{4} \lambda [ \{ \Gamma(\bar{k}) \}^2 - Z h_1^2 ] \quad (8b)$$

where  $Z$  is the lattice coordination number, and equal to 8 here. The index 1 of  $h_1$  indicates the hopping integral between the first nearest neighbors and  $\lambda$  is a parameter properly chosen. Model I corresponds to the usual nearest-neighbor tight-binding model which has been studied by many other authors. However, it has been pointed out that the magnitude of  $h_2$  is the same order as that of  $h_1$  in the bcc structure although it is negligible in the fcc and hcp structures.<sup>24</sup> This is due to the shorter distance of the next-nearest neighbors. Our new approximation (8b) is derived from the geometric feature of the CsCl-type lattice structure in order to take into account the higher-order hopping integrals. We can avoid  $\bar{k}$  dependence of the theory using this approximation. Keeping only the nearest-neighbor terms in  $\Gamma(\bar{k})$ , i.e.,

$$\Gamma(\bar{k}) = h_1 \sum_{j \in S_1} \exp(i\bar{k} \cdot \bar{r}_j) \quad (9)$$

(where the summation extends over the first shell of sites denoted by  $S_1$ ), we can express  $S(\bar{k})$  from Eq. (8b) as

$$\begin{aligned} S(\bar{k}) \approx & \lambda h_1^2 \sum_{j \in S_2} \exp(i\bar{k} \cdot \bar{r}_j) \\ & + \frac{1}{2} \lambda h_1^2 \sum_{k \in S_3} \exp(i\bar{k} \cdot \bar{r}_k) \\ & + \frac{1}{4} \lambda h_1^2 \sum_{l \in S_5} \exp(i\bar{k} \cdot \bar{r}_l) \quad (10) \end{aligned}$$

Therefore, if we set the value of  $\lambda$  to be equal to  $h_2/h_1^2$ , Eq. (10) gives the approximate sc dispersion relation which is equivalent to the special case such that

$$h_2 : h_3 : h_5 = 1 : \frac{1}{2} : \frac{1}{4} \quad (11)$$

This ratio cannot be changed as far as our approximation is used.

For the purpose of applying the CPA( $\eta$ ) to the present model, we must calculate the site-diagonal elements of the Green's function  $G_{\alpha\alpha}(z)$  and  $G_{\beta\beta}(z)$ . On a basis  $\langle n | = (\langle n\alpha |, \langle n\beta |)$ , the cell-diagonal element of the Green's function can be calculated in terms of Eqs. (6), (8a), and (8b)

$$\begin{aligned} \langle n | \hat{G}(z) | n \rangle &\equiv \begin{pmatrix} G_{\alpha\alpha}(z) & G_{\alpha\beta}(z) \\ G_{\beta\alpha}(z) & G_{\beta\beta}(z) \end{pmatrix} \\ &= \frac{1}{N} \sum_{\vec{k}} G[\Gamma(\vec{k}), z] \\ &= \frac{1}{N} \sum_{\vec{k}} \int_{-\infty}^{\infty} d\omega \delta[\omega - \Gamma(\vec{k})] G(\omega, z) \\ &= \int_{-\infty}^{\infty} d\omega g_0(\omega) G(\omega, z) , \quad (12) \end{aligned}$$

where

$$g_0(\omega) = \frac{1}{N} \sum_{\vec{k}} \delta[\omega - \Gamma(\vec{k})] . \quad (13)$$

Note that we may consider this  $g_0(\omega)$  the density of states of a nearest-neighbor tight-binding bcc metal, though the sum over  $\vec{k}$ 's is reduced to the inside of the sc Brillouin zone. Here,  $G[\Gamma(\vec{k}), z]$  depends on  $\vec{k}$  through both  $\Gamma(\vec{k})$  and  $\exp(i\vec{k} \cdot \vec{a})$ . Taking an average of the latter over all nearest-neighbor lattice vectors  $\vec{a}$ , we can also replace it by  $\Gamma(\vec{k})$ . This and the assumptions (8) assure  $\vec{k}$  independence of the self-energies. Thus, the last line of Eq. (12) is valid for  $G(\omega, z)$  calculated as

$$G(\omega, z) = \frac{1}{D(\omega, z)} \begin{pmatrix} z - \Sigma_{\beta} - \frac{1}{4}\lambda(\omega^2 - Zh_1^2) & -\omega^2 \\ -\omega^2 & z - \Sigma_{\alpha} - \frac{1}{4}\lambda(\omega^2 - Zh_1^2) \end{pmatrix} , \quad (14)$$

where

$$D(\omega, z) = [z - \Sigma_{\alpha} - \frac{1}{4}\lambda(\omega^2 - Zh_1^2)][z - \Sigma_{\beta} - \frac{1}{4}\lambda(\omega^2 - Zh_1^2)] - \omega^2 . \quad (15)$$

For model I,  $\lambda$  is taken to be zero. Explicit expressions for the components of Eq. (12) are obtained by evaluating the Hilbert transform of  $g_0(\omega)$  and we have (in energy units such that  $|Zh_1| = 1$ ), for model I,

$$G_{\alpha\alpha}(z) = \left[ \frac{z - \Sigma_{\beta}}{z - \Sigma_{\alpha}} \right]^{1/2} F_0(E) , \quad (16a)$$

$$G_{\beta\beta}(z) = \left[ \frac{z - \Sigma_{\alpha}}{z - \Sigma_{\beta}} \right]^{1/2} F_0(E) , \quad (16b)$$

$$G_{\alpha\beta}(z) = 1 - E \cdot F_0(E) , \quad (16c)$$

with

$$E = [(z - \Sigma_{\alpha})(z - \Sigma_{\beta})]^{1/2} \quad (17)$$

and

$$\begin{aligned} F_0(E) &= \frac{1}{N} \sum_{\vec{k}} \frac{1}{E - \Gamma(\vec{k})} \\ &= \int_{-\infty}^{\infty} d\omega \frac{g_0(\omega)}{E - \omega} . \end{aligned} \quad (18)$$

Here,  $F_0(E)$  is the Hilbert transform of  $g_0(\omega)$ . Similarly, for model II, we obtain

$$G_{\alpha\alpha}(z) = \frac{16}{\lambda^2(E_+^2 - E_-^2)} \left[ (z - \Sigma_{\beta} + \mu - \frac{1}{4}\lambda E_-^2) \frac{F_0(E_-)}{E_-} - (z - \Sigma_{\beta} + \mu - \frac{1}{4}\lambda E_+^2) \frac{F_0(E_+)}{E_+} \right] , \quad (19a)$$

$$G_{\beta\beta}(z) = \frac{16}{\lambda^2(E_+^2 - E_-^2)} \left[ (z - \Sigma_{\alpha} + \mu - \frac{1}{4}\lambda E_-^2) \frac{F_0(E_-)}{E_-} - (z - \Sigma_{\alpha} + \mu - \frac{1}{4}\lambda E_+^2) \frac{F_0(E_+)}{E_+} \right] , \quad (19b)$$

$$G_{\alpha\beta}(z) = \frac{16}{\lambda^2(E_+^2 - E_-^2)} [E_+ \cdot F_0(E_+) - E_- \cdot F_0(E_-)] , \quad (19c)$$

with

$$E_{\pm}^2 = \frac{2}{\lambda} \left[ (z - \Sigma_{\alpha} + \mu) + (z - \Sigma_{\beta} + \mu) + \frac{4}{\lambda} \pm \left[ (\Sigma_{\alpha} - \Sigma_{\beta})^2 + \frac{8}{\lambda} [(z - \Sigma_{\alpha} + \mu) + (z - \Sigma_{\beta} + \mu)] + \frac{16}{\lambda^2} \right]^{1/2} \right] \quad (20)$$

and

$$\mu = \frac{1}{4} \lambda h_1 = \frac{\lambda}{4Z} \quad (21)$$

Then, the effective site energies,  $\Sigma_\alpha$  and  $\Sigma_\beta$ , are determined from a system of two coupled equations<sup>12</sup> within the single-site approximation;

$$\Sigma_\alpha = \tilde{\Sigma}_\alpha - (\epsilon_A - \Sigma_\alpha)(\epsilon_B - \Sigma_\alpha) G_{\alpha\alpha}(\Sigma_\alpha, \Sigma_\beta, z) \quad (22a)$$

$$\Sigma_\beta = \tilde{\Sigma}_\beta - (\epsilon_A - \Sigma_\beta)(\epsilon_B - \Sigma_\beta) G_{\beta\beta}(\Sigma_\alpha, \Sigma_\beta, z) \quad (22b)$$

where  $\tilde{\Sigma}_\alpha$  ( $\tilde{\Sigma}_\beta$ ) is the average of site energies within the  $\alpha$  ( $\beta$ ) sublattice and given by

$$\tilde{\Sigma}_\alpha = \frac{1}{2}(1 + \eta)\epsilon_A + \frac{1}{2}(1 - \eta)\epsilon_B \quad (23a)$$

$$\tilde{\Sigma}_\beta = \frac{1}{2}(1 - \eta)\epsilon_A + \frac{1}{2}(1 + \eta)\epsilon_B \quad (23b)$$

Let us now extend the single-site CPA ( $\eta$ ) to include the effect of correlated scattering from a cluster caused by fluctuations and ordering. We will consider two kinds of clusters formed by a central atom and its first shell of atoms according as the central atom is at an  $\alpha$  or a  $\beta$  site. When the central atom is at an  $\alpha$  ( $\beta$ ) site, its nearest neighbors are all seated at  $\beta$  ( $\alpha$ ) sites in the CsCl-type lattice. The scattering from such a cluster is essentially described by a  $(Z + 1) \times (Z + 1)$   $T$  matrix and an effective medium in each sublattice is to be regarded as a  $(Z + 1) \times (Z + 1)$  matrix quantity. However, we replace the effective media by scalar effective site energies,  $\Sigma_\alpha(z)$  and  $\Sigma_\beta(z)$ , multiplied by the  $(Z + 1) \times (Z + 1)$  unit matrix according to the cluster CPA. Moreover, the scattering from a cluster is assumed to be characterized by the type of the central atom  $i$  and the number of  $A$  atoms in the shell ( $n$ ) approximately. These approximations simplify our numerical computation.

The system with an  $i(n)$  cluster embedded in effective media is described by the cluster Green's function. Its site-diagonal elements (at the central site) are given by

$$G_{\alpha\alpha}^{i(n)} = \frac{\Lambda_{\alpha\alpha}^{(n)}}{1 - (\epsilon_i - \Sigma_\alpha)\Lambda_{\alpha\alpha}^{(n)}} \quad (24a)$$

and

$$G_{\beta\beta}^{i(n)} = \frac{\Lambda_{\beta\beta}^{(n)}}{1 - (\epsilon_i - \Sigma_\beta)\Lambda_{\beta\beta}^{(n)}} \quad (24b)$$

for the respective kinds of clusters. We will modify the notations of Ref. 4 and rewrite the equations there to a convenient form for the present paper.  $\hat{\Lambda}^{(n)}$  is the Green's function describing the scattering from the shell. Hence,

$$\Lambda_{\alpha\alpha}^{(n)} = G_{\alpha\alpha} + G_{\alpha\beta}^2 \sum_{\beta, \beta' \in S_1} \tau_{\beta\beta'}^{(n)} \quad (25a)$$

and

$$\Lambda_{\beta\beta}^{(n)} = G_{\beta\beta} + G_{\beta\alpha}^2 \sum_{\alpha, \alpha' \in S_1} \tau_{\alpha\alpha'}^{(n)} \quad (25b)$$

$G_{\alpha\alpha}$ ,  $G_{\beta\beta}$ , and  $G_{\alpha\beta}$  have already been given in (16a ~ c) for model I and (19a ~ c) for model II. The subscripts  $\alpha$  and  $\beta$  are used as site indices instead of  $n\alpha$  and  $n\beta$  when we take the summation hereafter. The second term of Eqs. (25a) and (25b) the sum of  $T$ -matrix elements, is difficult to solve exactly, so that we decompose the  $T$  matrix into contributions over shell sites and replace them by their average value in the multiple-scattering equations<sup>25</sup> (see Ref. 4) to obtain

$$\sum_{\beta, \beta' \in S_1} \tau_{\beta\beta'}^{(n)} = \frac{Z \langle t_\beta / (1 + \Gamma_\beta t_\beta) \rangle}{1 - Z \Gamma_\beta \langle t_\beta / (1 + \Gamma_\beta t_\beta) \rangle} \quad (26a)$$

and

$$\sum_{\alpha, \alpha' \in S_1} \tau_{\alpha\alpha'}^{(n)} = \frac{Z \langle t_\alpha / (1 + \Gamma_\alpha t_\alpha) \rangle}{1 - Z \Gamma_\alpha \langle t_\alpha / (1 + \Gamma_\alpha t_\alpha) \rangle} \quad (26b)$$

where

$$t_\gamma = \frac{\epsilon_\gamma - \Sigma_\gamma}{1 - (\epsilon_\gamma - \Sigma_\gamma) G_{\gamma\gamma}} \quad (27)$$

and

$$\Gamma_\gamma = \frac{1}{Z-1} \sum_{\substack{\gamma' (\neq \gamma) \\ \gamma, \gamma' \in S_1}} G_{\gamma\gamma'} \quad (\gamma = \alpha \text{ or } \beta) \quad (28)$$

Expressions of  $\Gamma_\alpha(z)$  and  $\Gamma_\beta(z)$  are obtained from the diagonal matrix elements of the following  $2 \times 2$  matrix quantity  $\Gamma$ :

$$\begin{aligned} \Gamma &\equiv \frac{1}{Z-1} \sum_{\substack{n (\neq m) \\ n, m \in S_1}} \langle n | \hat{G}(z) | m \rangle \\ &= \frac{1}{Z-1} \sum_{\substack{n (\neq m) \\ n, m \in S_1}} \left[ \frac{1}{N} \sum_{\vec{k}} G[\Gamma(\vec{k}), z] \exp[i\vec{k} \cdot (\vec{r}_n - \vec{r}_m)] \right] \\ &= \frac{Z}{Z-1} \int_{-\infty}^{\infty} d\omega [g_0(\omega)(\omega^2 - Z^{-1})] G(\omega, z) \quad (29) \end{aligned}$$

Inserting Eqs. (6), (8a), and (8b) into Eq. (29), we can calculate by analogy with Eq. (12) and obtain, for model I,

$$\Gamma_\alpha(z) = \frac{Z}{Z-1} \left( \frac{z - \Sigma_\beta}{z - \Sigma_\alpha} \right)^{1/2} [E^2 F_0(E) - E - Z^{-1} F_0(E)] \quad (30a)$$

$$\Gamma_\beta(z) = \frac{Z}{Z-1} \left( \frac{z - \Sigma_\alpha}{z - \Sigma_\beta} \right)^{1/2} [E^2 F_0(E) - E - Z^{-1} F_0(E)] \quad (30b)$$

and for model II,

$$\Gamma_{\alpha}(z) = \frac{Z}{Z-1} \frac{16}{\lambda^2(E_+^2 - E_-^2)} \times \left[ (z - \Sigma_{\beta} + \mu - \frac{1}{4}\lambda E_-^2) \left( E_- F_0(E_-) - \frac{F_0(E_-)}{ZE_-} - 1 \right) - (z - \Sigma_{\beta} + \mu - \frac{1}{4}\lambda E_+^2) \left( E_+ F_0(E_+) - \frac{F_0(E_+)}{ZE_+} - 1 \right) \right] \quad (31a)$$

$$\Gamma_{\beta}(z) = \frac{Z}{Z-1} \frac{16}{\lambda^2(E_+^2 - E_-^2)} \times \left[ (z - \Sigma_{\alpha} + \mu - \frac{1}{4}\lambda E_-^2) \left( E_- F_0(E_-) - \frac{F_0(E_-)}{ZE_-} - 1 \right) - (z - \Sigma_{\alpha} + \mu - \frac{1}{4}\lambda E_+^2) \left( E_+ F_0(E_+) - \frac{F_0(E_+)}{ZE_+} - 1 \right) \right] \quad (31b)$$

Note that if  $\Sigma_{\alpha}$  and  $\Sigma_{\beta}$  are replaced by a single  $\Sigma$  in model I, its equations are reduced to those of Ref. 4. It should be emphasized that our theory depends only on the knowledge of  $F_0(E)$  in spite of taking into account the second- and higher-neighbor hopping integrals in model II.

The self-energies characterized by scalar quantities,  $\Sigma_{\alpha}$  and  $\Sigma_{\beta}$ , are now determined by a couple of self-consistent conditions:

$$G_{\alpha\alpha}(z) = \sum_{i,n} P_{\alpha}^{i(n)} G_{\alpha\alpha}^{i(n)}(z) \quad (32a)$$

$$G_{\beta\beta}(z) = \sum_{i,n} P_{\beta}^{i(n)} G_{\beta\beta}^{i(n)}(z) \quad (32b)$$

$P_{\alpha}^{i(n)}$  ( $P_{\beta}^{i(n)}$ ) is the probability of finding a cluster  $i(n)$  whose central atom is at an  $\alpha$  ( $\beta$ ) site. It is related to the LRO parameter  $\eta$  and the SRO parameter  $\sigma$  through

$$P_{\alpha}^{A(n)} = P_{\beta}^{B(Z-n)} = z C_n \frac{1}{2} (1 + \eta) \frac{(1 - \sigma)^n (1 + 2\eta + \alpha)^{Z-n}}{2^Z (1 + \eta)^Z} \quad (33a)$$

$$P_{\alpha}^{B(n)} = P_{\beta}^{A(z-n)} = z C_n \frac{1}{2} (1 - \eta) \frac{(1 - 2\eta + \sigma)^n (1 - \sigma)^{Z-n}}{2^Z (1 - \eta)^Z} \quad (33b)$$

We have already defined the LRO parameter  $\eta$  by Eq. (2) and here define the SRO parameter  $\sigma$  by

$$\sigma = \frac{N_{AB} - (N_{AA} + N_{BB})}{\frac{1}{2} Z N_0} \quad (34)$$

where  $N_{AB}$ ,  $N_{AA}$ , and  $N_{BB}$  denote the number of  $A-B$ ,  $A-A$ , and  $B-B$  bonds, respectively. However, we cannot determine the relation between  $\eta$  and  $\sigma$  uniquely.  $\eta$  can range between zero in the disordered state and 1 in the ordered state. When  $\eta$  is 1,  $\sigma$  is fixed at 1; otherwise, at a given value of  $\eta$ ,  $\sigma$  can take a value ranging from  $2\eta - 1$  to 1, in prin-

ciple. A negative value of  $\sigma$  indicates a tendency to segregate. In the case of pure LRO, in other words, when the distributions in the two sublattices are uncorrelated with each other, the relation between  $\eta$  and  $\sigma$  becomes

$$\sigma = \eta^2 \quad (35)$$

The deviation from this relation shows that short-range atomic correlation, clustering or ordering, is present.

Given a value of  $z$ , Eqs. (32a) and (32b) must be iterated until they converge to final values. As a starting value of iteration, it is convenient to use the result of CPA ( $\eta$ ).

### III. RESULTS AND DISCUSSION

We will calculate the electronic density of states per atom given by

$$g(E) = -\frac{1}{2\pi} \text{Im} [G_{\alpha\alpha}(z) + G_{\beta\beta}(z)]_{z=E+i0} \quad (36)$$

for several typical values of parameters. In this theory, model alloys are completely specified by only four dimensionless parameters  $\eta$ ,  $\sigma$ ,  $\delta (= \epsilon_A - \epsilon_B)$ , and  $\lambda$  or the ratio of the second to the first hopping integral  $h_2/h_1$ . It is convenient to choose the zero of energy in such a way that

$$\epsilon_A = -\epsilon_B = \frac{1}{2} \delta \quad (37)$$

and to scale in energy units such that  $|Zh_1| = 1$ . As previously noted, the knowledge of  $F_0(z)$  or  $g_0(E)$  (because  $F_0$  is obtained through the Hilbert transform of  $g_0$ ) is adequate for numerical evaluation. In this paper, we have performed the calculation of  $F_0(z)$  in two ways; one is an accurate but tedious calculation with the help of a continued-fraction technique and the other is an approximate calculation by substituting

$$F_0(z) = 2[z - (z^2 - 1)^{1/2}] \quad (38)$$

Here the latter corresponds to the case that all the continued-fraction coefficients are equal and gives a semicircular band. This will be useful to calculate a cohesive energy which is relatively insensitive to a band shape, especially when we take into account charge transfer self-consistently.

To use the semicircular band, the hopping integral  $h_1$  must be chosen so that the second moment of DOS agrees with that of the tight-binding model, i.e.,

$$Zh_1^2 = \frac{1}{4} . \quad (39)$$

From this choice of  $h_1$ , equations in Sec. II are slightly modified. It should be noted that in model II,  $F_0(z)$  and  $g_0(E)$  do not correspond to the unperturbed Green's function and the unperturbed density of states, respectively. In fact, the unperturbed density of states can be obtained from the theory with  $\delta=0$  and we show it in Fig. 1. Its energy range is easily evaluated to be

$$[-14|h_2| - 1, -14|h_2| + 1] \text{ for } h_2/h_1 \leq \frac{1}{4} \quad (40a)$$

and

$$[-14|h_2| - 1, 2|h_2| + 1/(64|h_2|)] \text{ for } h_2/h_1 \geq \frac{1}{4} . \quad (40b)$$

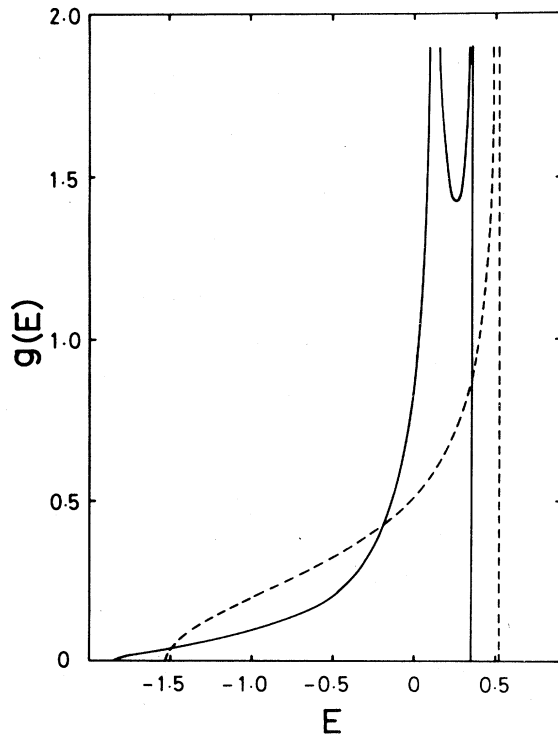


FIG. 1. Unperturbed density of states for model II as calculated by means of a continued-fraction expansion (solid line) and the semicircular DOS (broken line). The ratio of the second- to the first-neighbor hopping integral  $h_2/h_1$  is assumed to be 0.5 .

Now, we will present the numerical results and give brief discussion about them from three different points of view; long-range ordering, short-range ordering, and the band bottom.

### A. Long-range ordering

Our results for pure long-range ordering, obtained from the relation (35), are very close to those of the single-site CPA ( $\eta$ ) especially in the weak-scattering regime ( $\delta \leq 2$ ). This is due to the absence of short-range atomic correlation and the small cluster effects caused by fluctuations. In order to illustrate the effects of local environment, it is convenient to show the local density of states for each atom. The local density of states for an  $i$  atom in the  $\gamma$  sublattice surrounded by  $nA$  atoms and  $(Z-n)B$  atoms  $g_\gamma^{i(n)}(E)$  is given by

$$g_\gamma^{i(n)}(E) = -\frac{1}{\pi} \text{Im}[G_{\gamma\gamma}^{i(n)}(z)]_{z=E+i0} \quad (41)$$

in the present theory.

In Fig. 2, we quote the results for model I with the semicircular unperturbed density of states as simple examples mainly to facilitate their interpretation. It is clearly seen in Fig. 2(f) that the change in the total DOS curve (see, for instance, Fig. 1 of Ref. 14) is explained by  $g_\beta^{B(8)}$  and besides  $g_\alpha^{A(0)}$  which is symmetric with  $g_\beta^{B(8)}$  about  $E=0$ , because  $B(8)$  and  $A(0)$  clusters become more probable than the others as the degree of order increases. The sharp peaks of  $g_\alpha^{B(8)}$  [Fig. 2(e)] and  $g_\beta^{B(8)}$  curves correspond to the resonant level of an isolated  $B$  atom. They are not much affected by ordering and that of  $g_\beta^{B(8)}$  grows to be the lower main band in the perfectly-ordered state. When there is a slight deviation from perfect order, two impurity states appear between two main bands. From Fig. 2(a), the upper impurity state can be understood as arising from the impurity  $B$  atom in the  $\alpha$  sublattice. That is, this state turns out to be the antibonding state of the central  $B$  atom and the spherically symmetric shell of  $B$  atoms. Similarly, the lower impurity state corresponds to the antibonding state of an  $A$ -atom cluster.

As seen in Fig. 3, asymmetric total DOS curves can be successfully obtained for model II. The general look of their change differs much from that of model I. Direct comparison between models I and II is illustrated in Fig. 4. In fact, it can be pointed out the fact that an impurity state appears not only between but above the main bands. The two between the main bands correspond respectively to the antibonding states of an  $A$ -atom cluster and a  $B$ -atom cluster like model I. In addition, the one above the main bands corresponds to the bonding state of an  $A$ -atom cluster, which merges into the upper main band in model I. At the onset of ordering, a sharp peak aris-

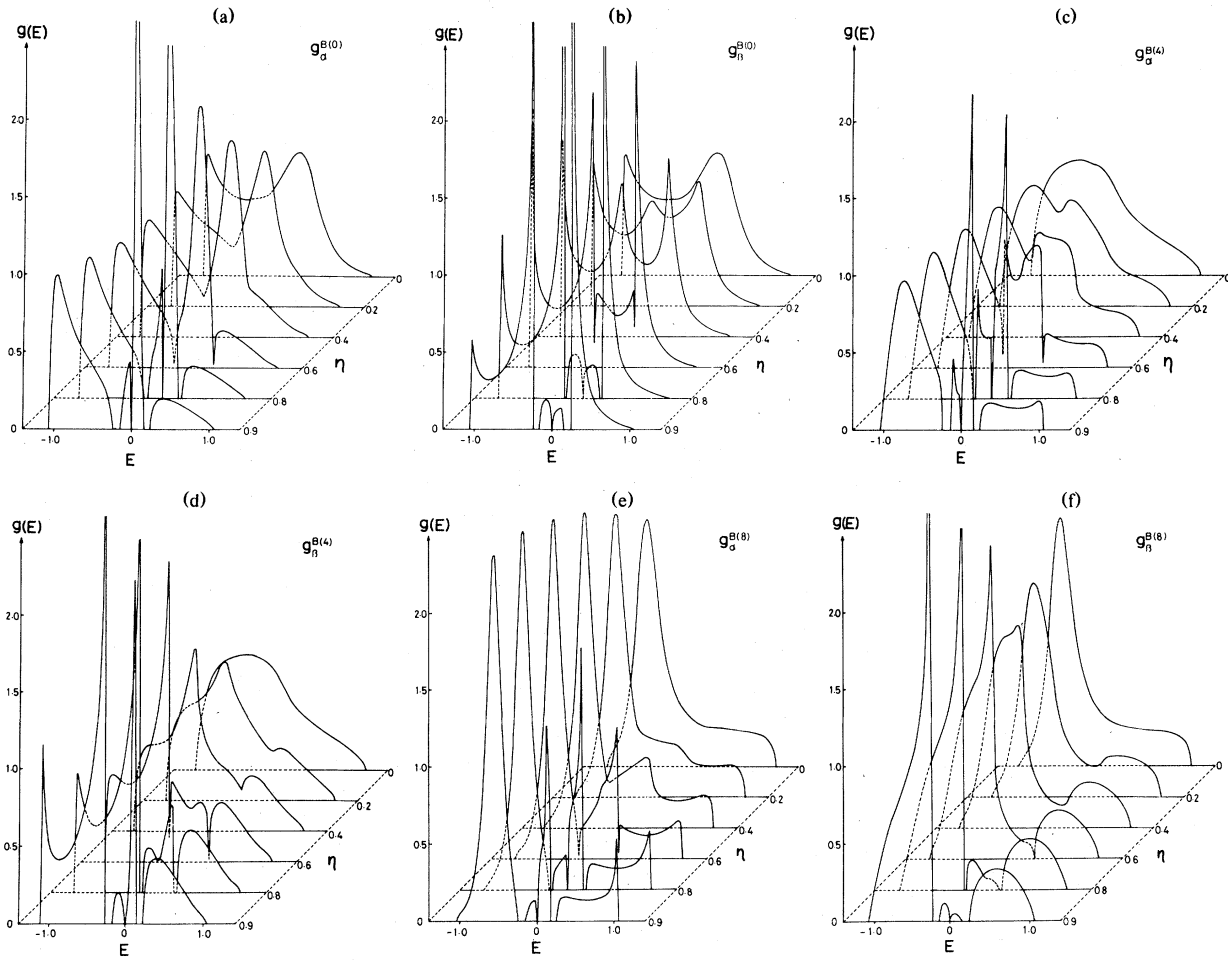


FIG. 2. (a)–(f) Some examples of the local density of states for a  $B$  atom in the  $\gamma$  sublattice surrounded by  $nA$  atoms and  $(Z - n)B$  atoms  $g_{\gamma}^{B(n)}(E)$  are plotted for several values of the LRO parameter  $\eta$ . Calculations are made for model I with the semicircular unperturbed DOS. The SRO parameter  $\sigma$  is set to be equal to  $\eta^2$  [see Eq. (29)] and  $\delta = 0.5$ .

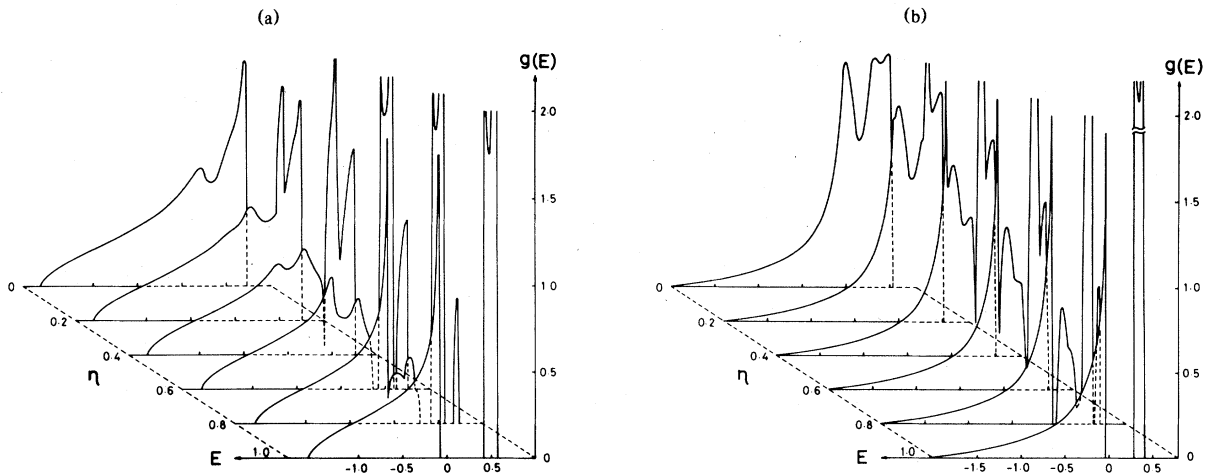


FIG. 3. Plot of the total density of states for model II ( $h_2/h_1 = 0.5$ ) in the case of long-range ordering ( $\sigma = \eta^2$ ). Calculations are made by means of (a) the semicircular band ( $\delta = 0.5$ ) and (b) a continued-fraction expansion ( $\delta = 0.35$ ).



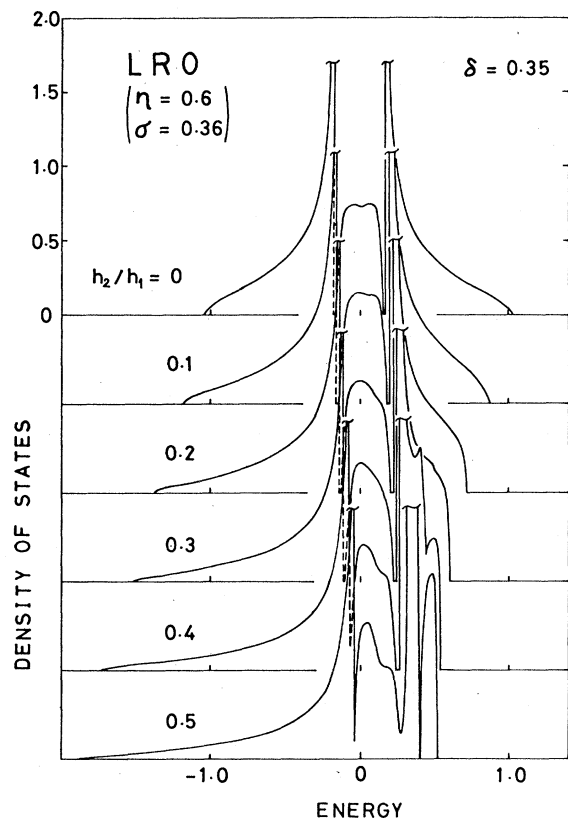


FIG. 4. Comparison between model I ( $h_2/h_1=0$ ) and model II ( $h_2/h_1=0.1, 0.2, 0.3, 0.4,$  and  $0.5$ ) in the case of long-range ordering ( $\eta=0.6, \sigma=0.36$ ). The total DOS is calculated for  $\delta=0.35$  with the help of a continued-fraction technique.

ing from the resonant level of an isolated  $A$  atom appears first and then gradually grows to be the upper main band. A peak for an isolated  $B$  atom appears soon after that and gives the upper limit of the lower main band. The behavior described above is easily interpreted in terms of local DOS's and this is a remarkable advantage of our theory.

### B. Short-range ordering

Here again we should emphasize the fact that short-range order is not independent of long-range order. In a partially long-range-ordered state, the presence of short-range atomic correlation is indicated by the deviation of  $\sigma$  from  $\eta^2$ . Therefore, it may be reasonable to regard short-range order as correction of long-range order.

As it is well known in the classical Bethe theory, after the long-range order has disappeared, the short-range order still remains. Let us investigate such a case in addition to the case that the system has a slight tendency to segregate. The results are shown in Fig. 5 for the values of  $\sigma$  ranging from  $-0.3$  to  $0.3$ , keeping  $\eta=0$  fixed. For larger absolute values of  $\sigma$ , convergence difficulty occurs mainly about the upper peak.

This indicates that the description by a site-diagonal coherent potential is less justified as the degree of short-range atomic correlation increases. Furthermore, it is believed to be unreasonable to regard such a system as microscopically homogeneous and replace it with uniform effective media. In the case of ordering, a peak arising from an isolated atom

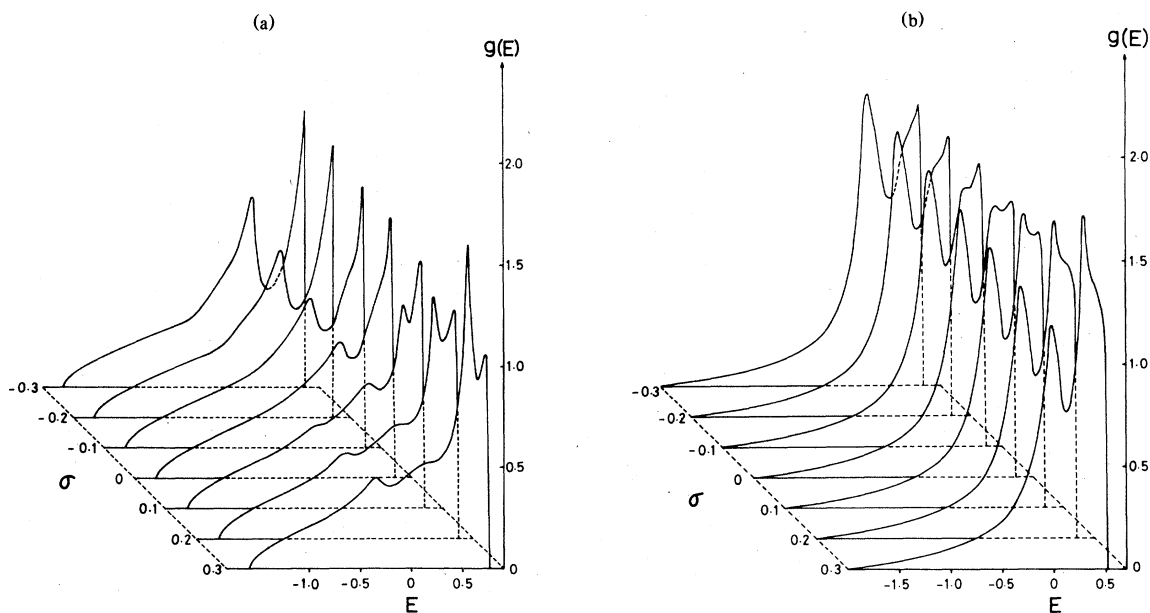


FIG. 5. Plot of the total density of states for model II ( $h_2/h_1=0.5$ ) in the case of short-range ordering and clustering ( $\eta=0$ ). Calculations are made by means of (a) the semicircular band ( $\delta=0.5$ ) and (b) a continued-fraction expansion ( $\delta=0.35$ ).

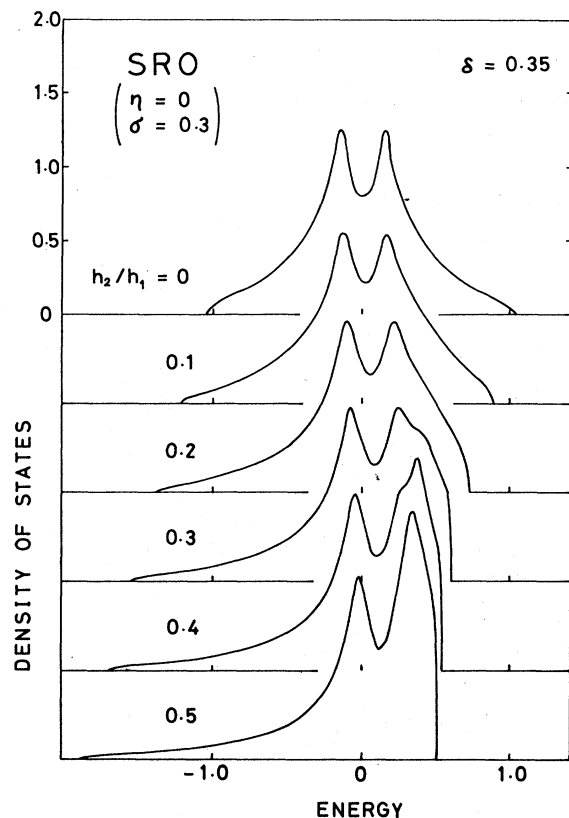


FIG. 6. Comparison between model I ( $h_2=0$ ) and model II ( $h_2/h_1=0.1, 0.2, 0.3, 0.4,$  and  $0.5$ ) in the case of short-range ordering ( $\eta=0, \sigma=0.3$ ). The total DOS is calculated for  $\delta=0.35$  with the help of a continued-fraction technique.

also appears, but it is slightly broadened and shifted compared with that of Fig. 3. In the case of clustering, the probability of finding  $A$ - and  $B$ -atom clusters increases and the corresponding peaks of antibonding state become larger. In the result, the total DOS curve seems to approach the arithmetical average of both constituent pure DOS curves with clustering. Comparison between models I and II is shown in Fig. 6.

### C. Band bottom

More-detailed results for the behavior of the band bottoms in Figs. 3(a) and 5(a) are given in Figs. 7 and 8, respectively. Figure 6 shows that the band edge moves towards higher- or lower-energy side according as  $\sigma > 0$  (ordering) or  $\sigma < 0$  (clustering), respectively. This tendency agrees with the calculation by Woolley and Mattuck<sup>26</sup> although their method is quite different from ours. Roughly speaking, the

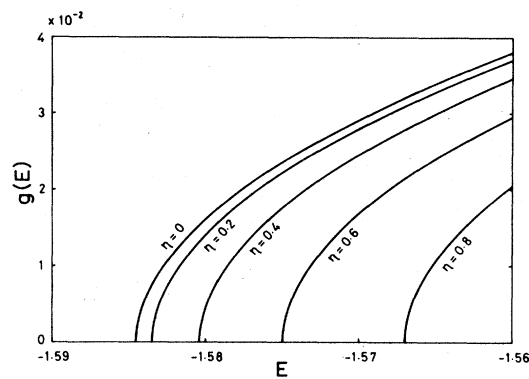


FIG. 7. Band bottoms of Fig. 3(a). The band edge moves towards higher-energy side approximately in proportional to  $\eta^2$ .

shift of the band edge if proportional to  $\eta^2$  in Fig. 7 and to  $\sigma$  in Fig. 8. This is of great interest in connection with the relation (35), because it suggests that the behavior of the band bottom is approximately determined by the value of the SRO parameter.

The lowest energy of the band bottom is considered to be determined by the localized levels in the largest regions of  $B$ -atom clusters. The probability of finding such a region is characterized by the number of  $B-B$  bonds provided that triple-site and other multisite correlations are not important. According to the definition of the SRO parameter (34), the number of  $B-B$  bonds is given by the value of the SRO parameter. Our observation is compatible with the above remarks.

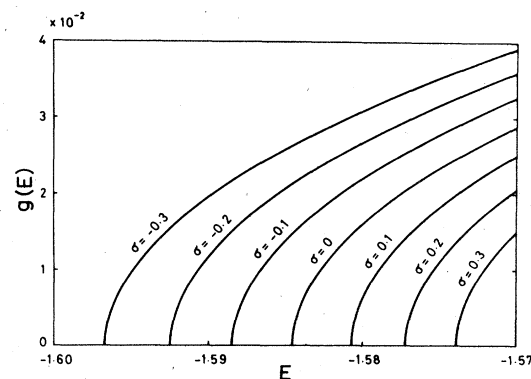


Fig. 8. Band bottoms of Fig. 5(b). The band edge moves towards higher- or lower-energy side according as  $\sigma > 0$  (ordering) or  $\sigma < 0$  (clustering) approximately in proportional to  $\sigma$ .

## IV. CONCLUSION

We have presented a new self-consistent method for studying the electronic structure in CsCl-type order-disorder alloys. For a better description of partially ordered states, we included both long- and short-range order parameters. The theory was based on a model with finite values of the second-neighbor hopping integral as well as the usual nearest-neighbor tight-binding model. The numerical results suggest that the inclusion of the second-neighbor hopping integral is quite important because DOS curves become asymmetric by that. Our method can produce reasonable DOS for all the range between the disordered state and the ordered state. As a result of numerical study over LRO and SRO parameter space, we found that the striking differences appeared according to the degree of order. This fact emphasizes that the effects of order should be investigated more intensively. We did not make any calculation for the strong-scattering regime because of the occurrence of unphysical behavior. In fact, convergence difficulties are observed chiefly for LRO and SRO parameter values

such that the deviation from the relation (35) is large. However, we feel that this failure cannot be attributed to the nonanalyticity problem mentioned before, because we did not encounter any nonanalytic behavior of the Green's function as far as perfect-disorder and pure-LRO cases are concerned, even in the strong-scattering regime ( $\delta \leq 6$ ). This analytic feature of our system justifies the present investigation, though this may depend on both its 50-50% concentration and its lattice structure. Quite recently, the authors have found that the convergence difficulties can be improved to a considerable extent, if consistency between a cluster and the external media is required not at the central site but at a boundary site of the cluster. Testing of the boundary-site approximation is now in progress.

In this paper, we have reported only the calculations for quite restricted cases. More explicit investigation over wider range of each parameter value and a comparison with other methods such as a generalization of the cluster-Bethe-lattice method<sup>14, 27, 28</sup> which can be applied to our problem will be made in a subsequent paper.

<sup>1</sup>P. Soven, Phys. Rev. 156, 809 (1967).

<sup>2</sup>M. Tsukada, J. Phys. Soc. Jpn. 26, 684 (1969).

<sup>3</sup>P. Dean, Proc. R. Soc. London Ser. A 254, 507 (1960); Rev. Mod. Phys. 44, 127 (1972).

<sup>4</sup>F. Brouers, F. Ducastelle, F. Gautier, and J. Van der Rest, J. Phys. F 3, 2120 (1973).

<sup>5</sup>H. Miwa, Prog. Theor. Phys. 52, 1 (1974).

<sup>6</sup>F. Brouers, F. Gautier, and J. Van der Rest, J. Phys. F 5, 975 (1975); J. Van der Rest, F. Gautier, and F. Brouers, *ibid.* 5, 995 (1975); J. Van der Rest, *ibid.* 7, 1051 (1977).

<sup>7</sup>W. H. Butler, Phys. Rev. B 8, 4499 (1973).

<sup>8</sup>B. G. Nickel and W. H. Butler, Phys. Rev. Lett. 30, 373 (1973).

<sup>9</sup>V. Kumar and S. K. Joshi, Phys. Rev. B 18, 2515 (1978).

<sup>10</sup>R. Alben and M. Blume, Phys. Rev. B 12, 4090 (1975).

<sup>11</sup>M. C. Desjonquères and F. Cyrot-Lackmann, J. Phys. F 7, 61 (1977).

<sup>12</sup>E. Ni Foo and H. Amar, Phys. Rev. Lett. 25, 1748 (1970).

<sup>13</sup>M. Plischke and D. Mattis, Phys. Rev. B 7, 2430 (1973).

<sup>14</sup>L. M. Falicov and F. Yndurain, Phys. Rev. B 12, 5664 (1975).

<sup>15</sup>T. Kaplan and L. J. Gray, Phys. Rev. B 15, 3260 (1977).

<sup>16</sup>P. Bloom and D. Mattis, Phys. Rev. B 15, 3633 (1977).

<sup>17</sup>C. T. White and E. N. Economou, Phys. Rev. B 15, 3742 (1977).

<sup>18</sup>D. G. Hall and J. S. Faulkner, Phys. Rev. B 15, 5850 (1977).

<sup>19</sup>F. Brouers, J. Giner, and J. Van der Rest, J. Phys. F 4, 214 (1974).

<sup>20</sup>J. Giner, F. Brouers, F. Gautier, and J. Van der Rest, J. Phys. F 6, 1281 (1976).

<sup>21</sup>H. Shiba, Prog. Theor. Phys. 46, 77 (1971).

<sup>22</sup>K. Niizeki, Prog. Theor. Phys. 53, 74 (1975).

<sup>23</sup>V. Kumar, D. Kumar, and S. K. Joshi, Phys. Rev. B 11, 2831 (1975).

<sup>24</sup>F. Ducastelle and F. Cyrot-Lackmann, J. Phys. Chem. Solids 31, 1295 (1970); M. C. Desjonquères and F. Cyrot-Lackmann, J. Phys. F 5, 1368 (1975).

<sup>25</sup>M. Lax, Rev. Mod. Phys. 23, 287 (1951).

<sup>26</sup>R. G. Woolly and R. D. Mattuck, J. Phys. F 3, 75 (1973).

<sup>27</sup>P. Chaudhuri and R. K. Moitra, Phys. Rev. B 18, 6694 (1978).

<sup>28</sup>R. C. Kittler and L. M. Falicov, Phys. Rev. B 18, 2506 (1978); 19, 291 (1979).